Journal of Alloys and Compounds, 191 (1993) 87–90
JALCOM 486

Phase relations in the SrO–SiO_2–ZrO_2 system
I. The system SrO–SiO_2

M. E. Huntelaar, E. H. P. Cordfunke and A. Scheele
Netherlands Energy Research Foundation ECN, Petten (Netherlands)

(Received August 10, 1992)

Abstract

The phase diagrams of the systems Sr_2SiO_4–$SrSiO_3$ and $SrSiO_3$–SiO_2 have been determined experimentally using differential thermal analysis. The eutectic compositions and temperatures of the Sr_2SiO_4–$SrSiO_3$ and $SrSiO_3$–SiO_2 subsystems are estimated to be 49.3 mol% SiO_2, 1840 K and 65.8 mol% SiO_2, 1615 K respectively. The enthalpy of fusion of $SrSiO_3$ has been measured to be 56 ± 6 kJ mol^{-1}.

1. Introduction

When during a severe nuclear reactor accident the core of the reactor melts, interactions of the fission products with the underlying concrete basemat are likely to occur. The formation of new compounds on reaction with the concrete will influence the release of less volatile, radiologically hazardous fission products such as barium or strontium. For this reason and because silica (SiO_2) is one of the main constituents of concrete, the phase diagram of the system SrO–SiO_2 is of particular interest.

Three compounds have been identified in this system: $SrSiO_3$, Sr_2SiO_4 and Sr_3SiO_5. The phase diagram of the system (or parts of it) has been determined by Eskola [1], Greig [2], Fields *et al.* [3] and Hageman and Oonk [4]. The investigations of Eskola and of Greig cover only the silica-rich side of the system. In addition, Hageman and Oonk measured the liquid immiscibility at this side of the system. Neither Eskola nor Greig was aware of the existence of Sr_3SiO_5, which was first reported by Nurse [5]. According to Eysel [6], Sr_3SiO_5(s) is not stable at room temperature but decomposes into SrO(s) and Sr_2SiO_4(s), similar to the CaO–SiO_2 system. Thermodynamic properties of this compound which could prove this are completely lacking.

The phase diagram analysis by Fields *et al.* covers only the strontium-oxide-rich side of the system. The liquidus curve of strontium oxide as proposed by these authors is not compatible with the melting point of strontium oxide reported by Noguchi [7] and Traverse and Foex [8]. Fields *et al.* adopted the measurements made by Eskola and by Greig for the silica-rich side to construct a phase diagram of the SrO–SiO_2 system.

Since the amount of strontium in irradiated nuclear fuel is small compared with the amount of silica present in the concrete, phase relations in the $SrSiO_3$–SiO_2 subsystem are of particular interest in nuclear technology. This system is insufficiently known and has therefore been (re)investigated in the present study.

2. Experimental details

The samples used in the differential thermal analysis (DTA) study have been prepared by mixing known amounts of Sr_2SiO_4(s) and $SrSiO_3$(s) or of $SrSiO_3$(s) and amorphous SiO_2(s) (Aldrich, 99.995% purity). The pure samples of Sr_2SiO_4(s) and $SrSiO_3$(s) are the same as used in ref. 9. All mixtures prepared for the $SrSiO_3$–SiO_2 subsystem were first partly melted at ±1625 K and then recrystallized at 1550 K in a purified argon atmosphere. Before and after each measurement the samples were analyzed by X-ray diffraction. In all mixtures containing SiO_2, cristobalite was found to be the crystalline phase at room temperature. In some of the mixtures with a high SiO_2 content, small traces of tridymite were found as well.

The DTA measurements were carried out in a Mettler TA 13-2000 apparatus using platinum crucibles. All measurements were made in a purified argon atmosphere to prevent the formation of volatile platinum oxides. The maximum temperature which can be obtained with the DTA furnace is 1873 K. The temperatures were corrected using the melting point of high purity palladium (1825 K) as a reference. Almost all measurements were reproducible within 3 K. The sensitivity of the DTA apparatus was calibrated against

0925-8388/93/$6.00

the enthalpies of fusion of silver, gold and palladium. The measurements were performed with ramp speeds between 1 and 25 K min^{-1}.

Quenching experiments were performed using a high temperature furnace. For each quenching experiment a platinum crucible was sealed in a partly evacuated (Ar pressure $\pm 10^4$ Pa), Al_2O_3-stabilized quartz capsule. Before quenching in ice water, the capsule was equilibrated for at least 45 min at the temperature of interest. The temperature was measured using a Pt/Pt–10%Rh thermocouple directly adjacent to the capsule.

Most handlings, such as weighing, were done in an argon-filled glove-box. All masses were corrected for buoyancy in argon.

3. Results

3.1. DTA measurements

The measured solidus and liquidus temperatures of the Sr_2SiO_4–$SrSiO_3$ and $SrSiO_3$–SiO_2 subsystems are listed in Table 1. Only a few points in the Sr_2SiO_4–$SrSiO_3$ subsystem could be measured because of the very high temperatures and the steep liquidus curve of Sr_2SiO_4. Temperatures on the SiO_2 branch of the $SrSiO_3$–SiO_2 system were difficult to measure owing to the relatively small enthalpy of fusion of SiO_2.

TABLE 1. Solidus and liquidus temperatures in the system SrO–SiO$_2$

Sample	SiO_2 (mol%)	T_{sol} (K)	T_{liq}[a] (K)
Sr_2SiO_4–$SrSiO_3$			
Sr/Si-53	47.50	1841	–
Sr/Si-52	48.07	1840	–
Sr/Si-86	49.00	1839	1861
Sr/Si-87	49.12	1839	1863
$SrSiO_3$–SiO_2			
Sr/Si-62	50.00	–	1853
Sr/Si-77	52.00	1619	1855
Sr/Si-72	54.06	1609	1833
Sr/Si-75	56.00	1614	1805
Sr/Si-70	58.28	1616	1767
Sr/Si-64	58.41	1614	1758
Sr/Si-65	58.96	1616	1751
Sr/Si-66	59.49	1610	1747
Sr/Si-71	60.61	1616	1722
Sr/Si-76	62.00	1619	1695
Sr/Si-67	64.39	1617	1654
Sr/Si-73	65.20	–	1632
Sr/Si-74	65.99	1617	–
Sr/Si-79	67.01	1618	–
Sr/Si-84	67.96	1614	–
Sr/Si-83	69.00	1616	1708
Sr/Si-85	69.50	1614	1739
Sr/Si-80	69.98	1615	1749
Sr/Si-81	71.01	1615	1760
Sr/Si-82	72.01	1621	1787

[a] All errors are within 1–3 K, except for the sample Sr/Si-85 where the liquidus temperature has an error of 18 K.

The melting temperature of pure $SrSiO_3$ was found to be 1853 ± 5 K, which is in excellent agreement with previous measurements by Jaeger and Van Klooster [10] (1851 ± 1 K), Eskola [1] (1853 ± 4 K) and Fields *et al.* [3] (1853 ± 15 K). For the melting temperature of $SrSiO_3$ the value 1853 ± 4 K is suggested.

3.2. Enthalpy of fusion

The enthalpy of fusion of $SrSiO_3$ was very difficult to obtain because the melting temperature lies only 20 K below the maximum obtainable temperature of our DTA apparatus. Another problem was the determination of the area under the melting peak. Owing to $\Delta_{\mathrm{fus}}C_{\mathrm{p}}$, the baseline leaps and therefore the peak area could not be determined unequivocally. Values between 50 and 62 kJ mol^{-1} were calculated depending on the calculational method applied. For the enthalpy of fusion of $SrSiO_3$ the value 56 ± 6 kJ mol^{-1} is therefore suggested.

3.3. Phase relations

The crystal structure of $SrSiO_3$ is monoclinic as reported by Machida *et al.* [11] and Marsh and Herbstein [12]. We found that on addition of even small amounts of SiO_2 the crystal structures became a little distorted, indicating that a small solubility area for SiO_2 may exist. The size of this solubility region has not been established in this study and so will be disregarded here.

In all our attempts to obtain tridymite as a stable phase, cristobalite was found as the major SiO_2 phase. Experiments were performed in which several mixtures of SrO(s) and SiO_2 were heated to 1573 K for a 240 h period. In these experiments tridymite was not found after slow cooling to room temperature. A similar experiment with CaO(s) and SiO_2 also yielded cristobalite only. This is in contrast to our experiments with SiO_2 and Na_2O, in which tridymite was readily obtained.

Quenching experiments at higher temperatures were performed with the sample Sr/Si-80 (molar ratio $SrO{:}SiO_2 = 0.4290$) to establish the phase relations at higher temperatures. A quenching experiment at 1600 K yielded tridymite, cristobalite and $SrSiO_3$ as the crystalline phases, whereas at 1640 K only tridymite could be found in the partially molten sample. Equilibria at still higher temperatures could not be measured because the capsules started to deform at 1640 K. The presence of tridymite in the quenched samples indicates that at higher temperatures the tridymite phase does exist. However, if mixtures are cooled down slowly from the same temperatures (1625–1640 K), only $SrSiO_3$, cristobalite and sometimes a small amount of tridymite are obtained.

It can be concluded from these experiments that although tridymite is formed in the liquid, the formation of cristobalite is kinetically more favourable. The presence of tridymite or cristobalite will, however, hardly effect the activities in the system, because the energy differences between the two phases are extremely small [13]. For this reason and because of the fact that tridymite is not a stable phase of pure (unstabilized) SiO_2 [14], the tridymite ↔ cristobalite transition (±1743 K) will be disregarded here.

4. Discussion

Our DTA measurements show that previous measurements in the $SrSiO_3$–SiO_2 system by Eskola and by Greig, who determined only a few points using a quenching method, are in fair agreement with the present results. According to our findings, the eutectic point in the $SrSiO_3$–SiO_2 system is situated at 1615 ± 3 K and 65.8 mol% SiO_2, which is only slightly different from the 1631 K and 66.49 mol% SiO_2 obtained by Eskola. In Fig. 1 a new phase diagram of th $SrSiO_3$–SiO_2 system is presented; the Sr_2SiO_4–$SrSiO_3$ system is given in the inset. The tridymite ↔ cristobalite transition temperature (1743 K) has been taken from the assessment of Wriedt [14].

In the Sr_2SiO_4–$SrSiO_3$ subsystem the eutectic point is found to be situated at approximately 1840 ± 3 K and 49.3 mol% SiO_2. These results are different from the results obtained by Eskola and by Fields *et al.*, who found 1818 K, 46.4 mol% SiO_2 and 1818 K, ±47 mol% SiO_2 respectively. The lower temperature found by Fields *et al.* can probably be explained by the use of the oxygen–acetelyne torch, which might have resulted in the formation of hydroxides.

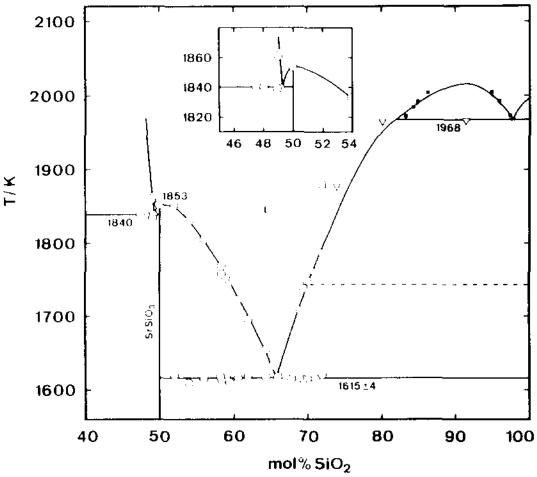

Fig. 1. The experimental phase diagram of the $SrSiO_3$–SiO_2 system. Inset: the eutectic region of the Sr_2SiO_4–$SrSiO_3$ phase diagram. Symbols: □, Eskola [1]; ▽, Greig [2]; ■, Hageman and Oonk [4]; ○, present study.

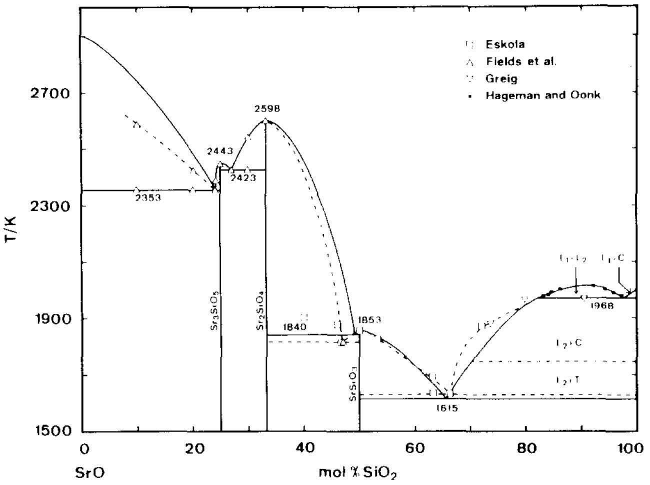

Fig. 2. The assessed phase diagram of the SrO–SiO_2 system: C, cristobalite; T, tridymite. The dashed lines indicate the previous phase equilibria.

TABLE 2. Melting points, eutectic temperatures and eutectic compositions in the system SrO–SiO_2

Compound	T_{melt} (K)	T_{eut} (K)	X_{eut} (mol% SiO_2)
SrO	2900		
Sr_3SiO_5	2443	2353	~23
Sr_2SO_4	2598	2423	~27
$SrSiO_3$	1853	1840	49.3
SiO_2	1996	1615	65.8

An assessed phase diagram of the whole SrO–SiO_2 system is given in Fig. 2. The liquidus measurements by Fields *et al.* on the SrO-rich side are possibly subject to errors, since they are in serious disagreement with the determinations of the melting point of SrO by Noguchi [7] (2872 ± 20 K) and Traverse and Foex [8] (2938 ± 20 K). We here select the value 2900 ± 40 K for the melting point of strontium oxide, *i.e.* the mean of the values of the latter two authors. A list of melting points, eutectic temperatures and eutectic compositions is given in Table 2.

References

1 P. Eskola, *Am. J. Sci., 5th Ser., 4* (1922) 331.
2 J. W. Greig, *Am. J. Sci., 5th Ser., 13* (1927) 1.
3 J. M. Fields, P. S. Dear and J. J. Brown, *J. Am. Ceram. Soc., 55* (1972) 585.
4 V. B. M. Hageman and H. A. J. Oonk, *Phys. Chem. Glasses, 27* (1986) 194.
5 R. W. Nurse, *J. Appl. Chem., 2* (1952) 244.
6 W. Eysel, *Neues Jahrb. Mineral. Monatsh., 23* (1970) 534.
7 T. Noguchi, *Adv. High Temp. Chem., 2* (1969) 235.

8 J. P. Traverse and M. Foex, *High Temp.-High Press.*, *1* (1969) 1409.
9 M. E. Huntelaar, E. H. P. Cordfunke and W. Ouweltjes, *J. Chem. Thermodyn.*, *24* (1992) 139.
10 F. M. Jäeger and H. S. Van Klooster, *Proc. K. Akad. Amsterdam*, *6* (1915) 896.
11 K. Machida, G. Adachi, J. Shiokawa, M. Shimida and M. Kazumi, *Acta Crystallogr. B*, *38* (1982) 386.
12 R. E. Marsh and F. H. Herbstein, *Acta Crystallogr. B*, *39* (1983) 280.
13 B. Hallstedt, *Calphad*, *16* (1992) 53.
14 H. A. Wriedt, *Bull. Alloy Phase Diag.*, *11* (1990) 43.